JOURNAL OF AIRCRAFT
Vol. 42, No. 5, September–October 2005

Engineering Notes

ENGINEERING NOTES are short manuscripts describing new developments or important results of a preliminary nature. These Notes should not exceed 2500 words (where a figure or table counts as 200 words). Following informal review by the Editors, they may be published within a few months of the date of receipt. Style requirements are the same as for regular contributions (see inside back cover).

Automatic Transition Prediction for High-Lift Systems Using a Hybrid Flow Solver

Andreas Krumbein*
DLR, German Aerospace Center, D-38108 Brunswick, Germany

I. Introduction

THE modeling of laminar–turbulent transition in Reynolds averaged Navier–Stokes (RANS) solvers is a necessary requirement for the computation of flows over airfoils and wings in the aerospace industry because it is not possible to obtain quantitatively correct results if laminar–turbulent transition is not taken into account. For the design process of wings in industry, there exists the demand for a RANS-based computational fluid dynamics tool that is able to handle flows with laminar–turbulent transition automatically and autonomously. The first steps toward the setup of such a tool were made, for example, in Ref. 1, where a structured RANS solver and an e^N method[2,3] were applied, and in Ref. 4, where a RANS solver, a laminar boundary-layer method,[5] and an e^N method were coupled. There, the boundary-layer method was used to produce highly accurate laminar, viscous layer data to be analyzed by a linear stability code. The use of an e^N-database method[6] results in a coupled program system that is able to handle transition prediction automatically. In Ref. 7, a database for the growth rates is used that are represented by a trained neural network based on Falkner–Skan–Cooke profiles. Alternative approaches using a transition closure model or a transition/turbulence model directly incorporated into a RANS solver are documented in Refs. 8–10.

Because the block-structured RANS solver FLOWer[11] has been brought to a well-engineered state with regard to automatic transition prediction and transitional flow modeling,[12–15] the hybrid RANS solver TAU[16] was extended in a similar way to combine the benefits of a hybrid RANS code with an automatic transition prediction capability,[17] in the form of the DLR, German Aerospace Center transition prediction module.[12–15]

The TAU code solves the three-dimensional compressible RANS equations using unstructured/hybrid grids, which may consist of hexahedral, tetrahedral, pyramidal, and prismatic cells and, therefore, combine the advantages of regular grids for the accurate resolution of viscous shear layers in the vicinity of walls with the flexibility of grid-generation techniques for unstructured grids. The use of a dual grid makes the solver independent of the type of cells that compose the initial grid. In this study, a central spatial discretization scheme with scalar artificial dissipation and a multigrid procedure for convergence acceleration was used. The integration in time is performed using an explicit multistage time-stepping scheme.

In this Engineering Note, the first application of the coupled system consisting of the hybrid TAU code and the transition prediction module to a high-lift multi-element configuration is presented. The coupling of the TAU code and the transition prediction module and the transition prediction strategy are outlined, and it is shown that the results of the transition prediction procedure are independent of the type of the RANS solver (structured or hybrid). On the other hand, the final results from the RANS solver turn out to be strongly dependent on the flow solver itself. In a comparison with results obtained with the FLOWer code, significant differences may occur, although the spatial discretization schemes are the same, the discretization of the governing equations is based on the same approach, and the parameters of the artificial dissipation and the turbulence models used are the same for the computations of the same configuration with the two different codes. Also the different structures and point distributions and resolutions of the two computational grids can not explain all of the observed differences. Both show the independence of the results of the transition prediction approach regardless of which flow solver is used and to point out that, at the same time, the flow results may depend strongly on the flow solver itself while the values of the transition locations are the same for both codes is the main objective of this work.

Another objective is to show the high potential of using a laminar boundary-layer method between the RANS solver and the e^N-database method instead of using the boundary-layer parameters computed directly from the RANS grid. Whereas in Refs. 17–19 the boundary-layer parameters were computed directly from the RANS grid, here a laminar boundary-layer method was used to provide highly accurate boundary-layer data. In so doing, the computation time can be massively reduced. In Refs. 18 and 19, an extensive sensitivity study is documented where settings of the coupling parameters were found that allow for a fast and accurate iteration of the transition locations.

It is shown that fast and accurate predictions of the transition locations are possible for a high-lift system using a computational grid that is of a type typically used in practical industrial applications and that was designed without accounting for the accuracy of the transition locations. This is a consequence of using a laminar boundary-layer method for the computation of the viscous data required by the e^N method. The computational results are compared to those obtained with the FLOWer code and to experimental findings.

II. Coupling of the RANS Solver and the Transition Prediction Module

The transition prediction module consists of a laminar boundary-layer code for swept, tapered wings[5] and an e^N-database method for Tollmien–Schlichting (TS) instabilities (see Ref. 6). The coupled system can be run in two different modes. Either the TAU code communicates the surface pressure distribution of the configuration to the laminar boundary-layer method, the laminar boundary-layer method then computes all of the boundary-layer parameters that are needed for the e^N-database method, and the e^N-database method determines new transition locations that are given back to the RANS solver (first mode), or the TAU code computes the necessary boundary-layer parameters, δ, H_i, and Reynolds number

Received 18 February 2005; revision received 18 April 2005; accepted for publication 18 April 2005.

*Research Scientist, Design Engineer, Institute of Aerodynamics and Flow Technology, Numerical Methods; Lilienthalplatz 7; andreas.krumbein@dlr.de. Member AIAA.

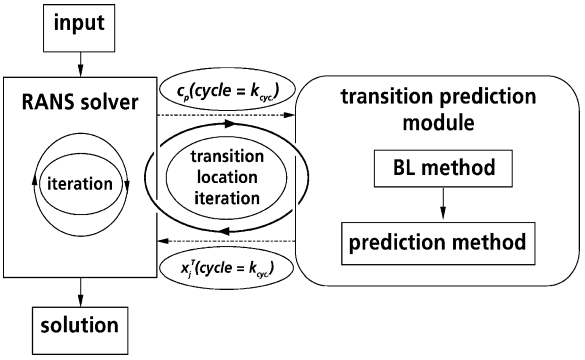

Fig. 1 Coupling structure of RANS solver and transition prediction module.

Re_{δ^*}; internally and communicates them directly to the e^N-database method (second mode). In Ref. 17, the influence of the cell number in wall normal direction and a comparison with results from a boundary-layer code are shown.

This coupled structure results in an iteration procedure for the transition locations within the iterations of the RANS equations. The structure of the approach using the first mode is outlined graphically in Fig. 1. After a certain number of iterations, k_{cyc}, of the RANS solution process, the solver is stopped, the transition prediction module is called, and the module analyzes the laminar boundary layers of the upper and lower sides of an airfoil configuration and determines transition locations x_j^T (cycle $= k_{\mathrm{cyc}}$), $j = 1, \ldots, n_{\mathrm{elem}}$, where n_{elem} is the number of transition points. These locations are communicated back to the RANS solver, and the computation is continued. In so doing, the determination of the transition locations becomes an iteration process itself. At every call of the module, the surface pressure c_p(cycle $= k_{\mathrm{cyc}}$) or the internally computed boundary-layer parameters along the surface of an airfoil are used as input for the transition prediction module. The viscous data are subsequently analyzed by the e^N-database method. The algorithm for the transition prediction iteration works as follows.

1) The RANS solver is started as if a computation with prescribed transition locations is to be performed. At this stage, the transition locations are set very far downstream on the upper and lower sides of the airfoil, for example, at the trailing edge. The RANS solver then initially computes a fully laminar flow or a flow with large laminar regions over the airfoil.

2) During the solution process of the RANS equations, the laminar flow regions are checked for laminar separation points by the RANS solver. In the case that laminar separation is detected, the separation point is used as an approximation of the transition location and the computation is continued.

3) The RANS equations are iterated until the lift coefficient $c_l = c_l$(cycles) has become constant with respect to the iteration cycles.

4) The transition prediction module is called. The e^N-database method determines the transition locations on upper and lower sides of the airfoil. The procedure acts differently in the first mode and in the second mode. In the case that the e^N-database method does not detect a transition location due to TS waves, two possibilities are implemented: Either the laminar separation point from the boundary-layer code is used as an approximation of the transition point (first mode) or the previous transition locations is kept unchanged (second mode).

5) The current coordinate $x_j^T(k_{\mathrm{cyc}})$, which is used as transition location, is underrelaxed. That is, as new transition locations, the coordinates $x_j^{*T}(k_{\mathrm{cyc}})$, which are located downstream of the coordinates x_j^T, are used according to $x_j^{*T}(k_{\mathrm{cyc}}) = C_j^T(k_{\mathrm{cyc}}) x_j^T(k_{\mathrm{cyc}})$, $j = 1, \ldots, n_{\mathrm{elem}}$, and $C_j^T(k_{\mathrm{cyc}}) > 1$. Only after the last step of the transition location iteration, $C_j^T(k_{\mathrm{cyc}}) = 1$ is applied. For the value of the underrelaxation factor $C_j^T(k_{\mathrm{cyc}}) = C_j^T(k_{\mathrm{cyc}}^l) = x_j^T(k_{\mathrm{cyc}}^l) + C^{T,\mathrm{init}} |x_j^{*T}(k_{\mathrm{cyc}}^{l-1}) - x_j^T(k_{\mathrm{cyc}}^l)|$ is used, where l is the current iteration step and $C^{T,\mathrm{init}}$ is an initial value of the underrelaxation factor given as input parameter by the user of the code. In the case that the convergence criterion from step 6 is satisfied, $C_j^T(k_{\mathrm{cyc}}) = 1$ is applied.

6) As convergence criterion, $\Delta x_j^{*T,l} < \varepsilon \approx 1\%$ with $\Delta x_j^{*T,l} = |x_j^{*T}(k_{\mathrm{cyc}}^l) - x_j^{*T}(k_{\mathrm{cyc}}^{l-1})|$ is applied. In the case that the criterion is satisfied, the iteration for x_j^T is finished, otherwise the algorithm loops back to station 2.

III. Results

The coupled system was applied to the same two-dimensional takoff configuration of a representative civil aircraft[20] as used in Ref. 14. At $M = 0.22$, $Re = 6 \times 10^6$, and $\alpha = 21.4$ deg, the limiting N factor for the TS-database method, $N_T = 9$, according to Arthur et al.,[21] and the Spalart–Allmaras one-equation turbulence model,[22] with Edwards and Chandra modification[23] Spalart-Allmaras-Edwards (SAE), were used. The following transition locations were determined[20] experimentally on the upper sides of the slat $(x_{\mathrm{upp}}^T/c)_{\mathrm{slat}} = 0.15$, and on the flap $(x_{\mathrm{upp}}^T/c)_{\mathrm{flap}} = 0.345$. On the main airfoil upper side, the transition location was not measured, but the location of the upper side kink, the point where the slat trailing edge is located when the configuration is undeflected, may be useful as a point of orientation, $(x_{\mathrm{upp}}^{\mathrm{kink}}/c)_{\mathrm{main}} = 0.19$. On the lower sides, the transition points were not measured, and for the computation, fully laminar flow is assumed.[15] Figure 2 shows the computational grid, which is of a type typically used in practical applications and consists of about 22,000 grid points, which form about 6900 triangles and about 18,200 quadriliterals. The slat surface is resolved with 124 points, the main airfoil with 290 points, and the flap surface with 172 points. The computation was started with initial transition locations set at 75% of the chords of the three elements on the upper sides. The transition location iteration was done only for the upper sides of the three elements.

The basic parameter settings for the coupling procedure were the overall number of iteration cycles for the RANS computation, $\mathrm{cycle}_{\max} = 15,000$, and the cycle interval for the iteration of the transition locations, $\Delta k_{\mathrm{cyc}} = 1000$. A converged fully turbulent restart solution of the flowfield was used as initial condition to accelerate the computation with transition prediction. In so doing, it is assured that the computation with transition prediction does not produce large disturbances at the beginning of the transient phase, which might hinder convergence of the RANS iterations. In any case, at the beginning of the computation, a solution with large laminar portions is computed because the initial transition locations are set far downstream. The initial conditions have almost no effect on the transition prediction process.

The transition prediction procedure was run in the first mode because, in the structured part of the hybrid grid whose outer edge is located far from the surface, the number of cells in wall the normal direction is not sufficiently large, only 48, to compute highly accurate boundary-layer data and the grid lines do not run well perpendicularly from the surface.

In Fig. 3, the overall convergence of the RANS computation is shown. The starting values of the curves represent the final values of the fully turbulent restart solution. After a strong perturbation at

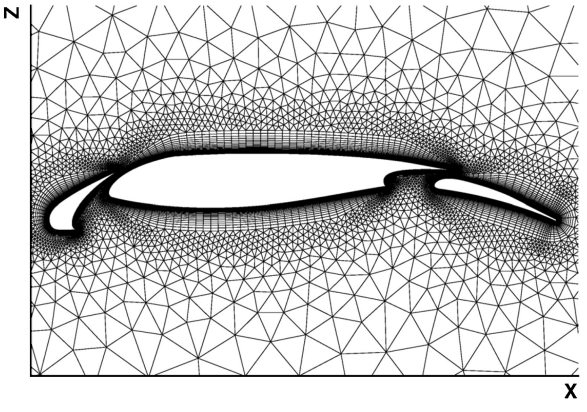

Fig. 2 Hybrid grid.

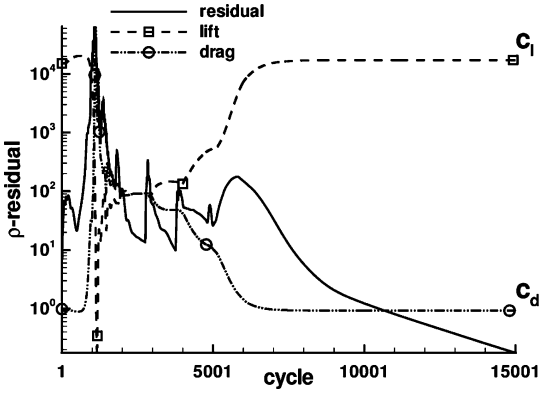

Fig. 3 Convergence history of RANS computation.

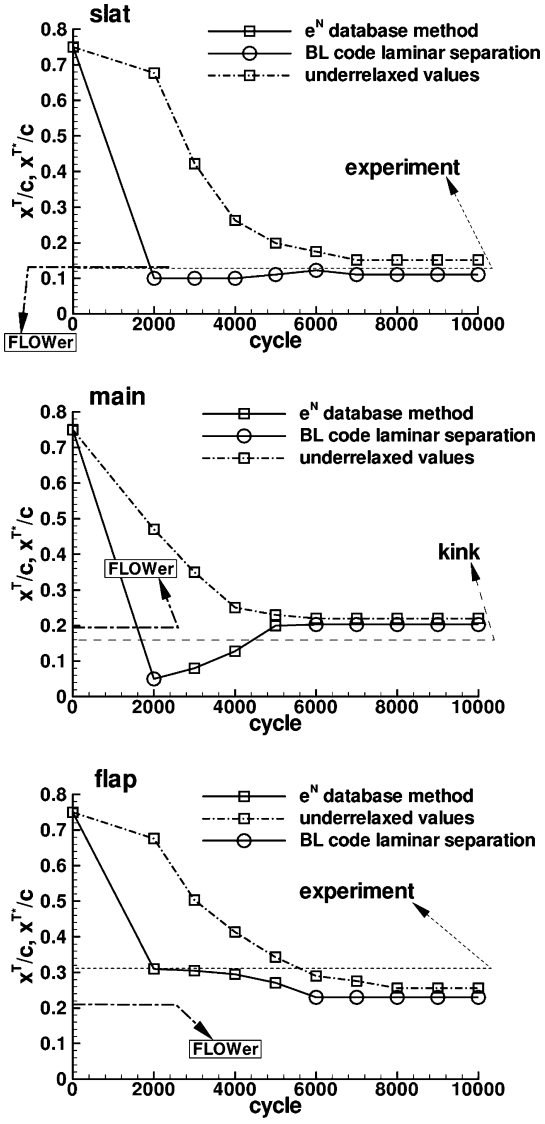

Fig. 4 Convergence histories of transition location iteration at three elements.

cycle ≈ 1100, the computation converges very smoothly to a steady state, affected only by the change of the transition location values and only as long as the transition locations have not yet converged. The first call of the transition prediction module was carried out at cycle $= 2000$, and the force coefficients have converged after about 8000 RANS cycles and 7 calls of the transition prediction module. Laminar separations in the RANS computational grid did not occur.

In Fig. 4, the convergence histories of the transition location iterations for the three elements are shown. The transition locations, which were directly determined by the e^N-database method, are shown as solid lines with square symbols. The transition locations are shown as solid lines with hollow circles when a laminar separation point from the laminar boundary-layer code was used as approximation of the transition point. The values of the underrelaxed transition locations (dash–dotted lines with square symbols) have converged on all three elements after 8000 RANS cycles. On the slat, the converged underrelaxed transition point, which remains a bit downstream of the laminar separation point from the boundary-layer code, is located about 2% downstream of the experimental value. At the main airfoil, the converged underrelaxed transition point is located about 6% downstream of the upper side kink position, and at the flap, the converged underrelaxed transition point is located about 5.7% too far upstream compared with the transition location from the experiment based on the following specification of $b\% = [(x^T_{\text{comp}} - x^T_{\text{exp}})/c]_{\text{elem}}$, where elem is the slat, main, or flap. The converged transition locations on all three elements are based on laminar separation points from the boundary-layer method, that is, the underrelaxed values of the laminar separation points from the boundary-layer method are used as approximations for the real transition points. During the transition location iteration, the e^N-database method yielded results for the main airfoil in the second, third, and fourth call of the transition prediction module and in the first to fourth call for the flap. In the other cases, no transition points could be computed before the laminar boundary layer separates.

The same character of the converged transition locations was found when the test case was computed with the FLOWer code using the same turbulence model.[15] The accuracy of the predicted transition locations in this case is of the same high quality as in Ref. 15. The differences between the values with and without underrelaxation remain in the depictions in Fig. 4, because the transition locations without underrelaxation are located between two surface grid points.

A comparison of the transition locations computed with the two different coupled systems shows that all transition locations from the TAU computation are located slightly downstream of those from the FLOWer computation. This is due to the different surface point distributions in the two different grids and due to the coarser circumferential surface resolution in the hybrid grid. However, the final values of the transition locations without underrelaxation from the FLOWer computation in Ref. 15 and the corresponding values in this presentation are identical due to the use of the boundary-layer method.

These results show the high potential of using a laminar boundary-layer method between the RANS solver and the e^N database method instead of using the boundary-layer parameters computed directly from the RANS grid as it was done in Refs. 17–19. In so doing, the RANS cycle interval between two consecutive calls of the transition prediction module could be reduced by 60%, yielding accurate approximations of the transition locations. In so doing, it was possible to reduce the overall computational effort significantly by a strong reduction of the number of RANS cycles needed to obtain a steady-state solution.

For the flap transition location, one may assume that the transition occurs inside a laminar separation bubble so that the current approach is not sufficient to yield a better approximation than the one presented. A transition prediction approach that is able to detect the transition point downstream of the point of laminar separation, for example, an empirical criterion, is needed here.

The comparison of the c_p distributions in Fig. 5 shows a very good matching of the TAU results with the measured curves[20] and the FLOWer results based on the Wilcox k–ω turbulence model.[24] The differences between the two results from the computations using the SAE model are remarkable. The FLOWer result using the SAE model clearly underpredicts the pressure levels on the suction sides of all three elements and the suction peak on the slat is not reached, although the transition locations are almost the same, as shown earlier.

Figure 6 shows the comparison of the computed c_f distributions. Here one can see clearly that the FLOWer solution using the SAE model is strongly affected by a large separation at the main element trailing edge. This separation does not occur in either the FLOWer

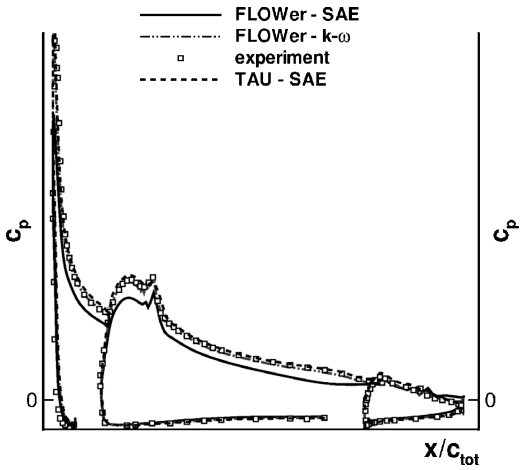

Fig. 5 Computational results from FLOWer and TAU and experiments: c_p distributions.

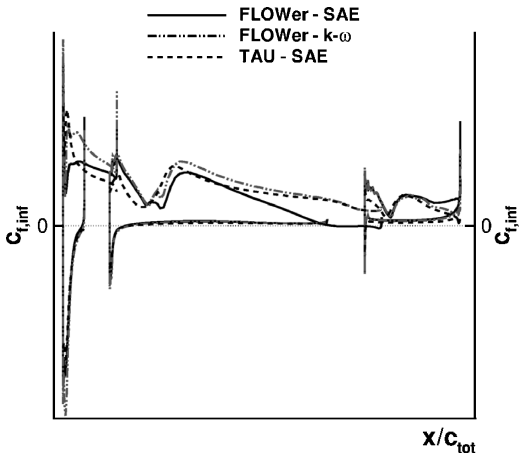

Fig. 6 Computational results from FLOWer and TAU: c_f distributions.

solution using the Wilcox k–ω model or the TAU solution using the SAE model. In the TAU solution, the rise of the skin friction in the transition region starts farther upstream than in the FLOWer solution on all three elements, which can be seen clearly in the c_f distributions of the main element and the flap. On the main element, the c_f distributions of the FLOWer computations are characterized by a small dip in the transition region around the upper side kink, whose effect is clearly visible as a strong oscillation in all c_p distributions. This dip does not occur in the TAU solution. A remarkable difference between the FLOWer solutions and the TAU solution is the different levels of the skin-friction in the laminar parts of the flow. The skin-friction levels of the c_f distributions obtained with the TAU code are significantly lower than those from the FLOWer computations. All computations were carried out applying point transition on all three elements.

The causes for these differences are not yet understood. Further investigations are necessary to quantify the impact of a hybrid grid having more points on the surfaces and providing a better resolution of the boundary layer. Moreover, the postprocessing procedures used to evaluate the skin friction must be compared in detail.

Finally, the influence of different transitional flow models must be tested so that the comparison with the FLOWer results can be completed.

IV. Conclusions

The hybrid TAU code coupled to a transition prediction module was successfully applied to a high-lift multi-element configuration while automatically taking into account the transition locations that were predicted by an e^N-database method or were based on laminar separation points determined by a laminar boundary-layer code. The experimentally measured transition locations could be determined with very high accuracy, although the test case was run on a computational grid with only sparse resolution in the wall normal direction, as well as in circumferential direction in the structured part of the hybrid grid, which is of a grid type typically used in practical industrial applications and which was designed without accounting for the accuracy of the transition locations. This result shows the high potential of using a laminar boundary-layer method between the RANS solver and the e^N-database method instead of using the boundary-layer parameters computed directly from the RANS grid. By this method, the RANS cycle interval between two consecutive calls of the transition prediction module could be reduced by 60%, yielding accurate approximations of the transition locations. Thus, it was possible to reduce the overall computational effort significantly by a strong reduction of the number of RANS cycles needed to obtain a steady-state solution.

It was shown that the results of the transition prediction procedure for the test case investigated are independent of the type of the RANS solver (structured or hybrid). A comparison between the results of the hybrid RANS code and those of a block-structured RANS code, however, shows that the final results from the RANS solver can depend strongly on the flow solver itself, although the values of the transition locations are almost the same for both codes. In the comparison, significant differences occur although the spatial discretization schemes are the same, the discretization of the governing equations is based on the same approach, and the parameters of the artificial dissipation and the turbulence models used are the same with the two different codes. To quantify the impact of a hybrid grid having more points on the surfaces and providing a better resolution of the boundary layer further investigation is necessary.

Acknowledgments

This work has been carried out within the European Project High Level Modelling of High Lift Aerodynamics (HiAer) and is documented in detail in Ref. 18. The project was managed by the Totalförsvarets Forskningsinstitut (FOI, Swedish Defence Research Agency) in Sweden and was partly funded by the European Union (Project Reference G4RD-CT-2001-00448). The HiAer project was a collaboration between DLR in Germany, the Office National d'Études et de Recherches Aérospatiale (ONERA, French Aeronautics and Space Research Center) in France, the Kungliga Tekniska Högskolan (KTH, Royal Institute of Technology) in Sweden, the Helsinki University of Technology (HUT) in Finland, the Technical University of Berlin (TUB) in Germany, Alenia in Italy, Airbus Deutschland in Germany, QinetiQ in Great Britain and FOI. We acknowledge BAE Systems for letting us use the 59% section data of a representative civil aircraft wing in this study.

References

[1]Radespiel, R., Graage, K., and Brodersen, O., "Transition Predictions Using Reynolds-Averaged Navier–Stokes and Linear Stability Analysis Methods," AIAA Paper 91-1641, June 1991.

[2]Smith, A. M. O., and Gamberoni, N., "Transition, Pressure Gradient and Stability Theory," Douglas Aircraft Co., Rept. ES 26388, Long Beach, CA, Aug. 1956.

[3]van Ingen, J. L., "A Suggested Semi-Empirical Method for the Calculation of the Boundary Layer Transition Region," Dept. of Aerospace Engineering, Rept. VTH-74, Univ. of Delft, Delft, The Netherlands, Oct. 1956.

[4]Stock, H. W., and Haase, W., "A Feasibility Study of e^N Transition Prediction in Navier–Stokes Methods for Airfoils," *AIAA Journal*, Vol. 37, No. 10, 1999, pp. 1187–1196.

[5]Horton, H. P., and Stock, H. W., "Computation of Compressible, Laminar Boundary Layers on Swept, Tapered Wings," *Journal of Aircraft*, Vol. 32, No. 6, 1995, pp. 1402–1405.

[6]Stock, H. W., and Degenhardt, E., "A Simplified e^N Method for Transition Prediction in Two-Dimensional, Incompressible Boundary Layers," *Zeitung für Flugwissenschaft und Weltraumforschung*, Vol. 13, No. 1, 1989, pp. 16–30.

[7]Crouch, J. D., Crouch, I. W. M., Ng, L. L., "Transition Prediction for Three-Dimensional Boundary Layers in Computational Fluid Dynamics Applications," *AIAA Journal*, Vol. 40, No. 8, 2002, pp. 1536–1541.

[8]Warren, E. S., and Hassan, H. A., "Transition Closure Model for Predicting Transition Onset," *Journal of Aircraft*, Vol. 35, No. 5, 1998, pp. 769–775.

[9]Czerwiec, R. M., Edwards, J. R., Rumsey, C. L., Bertelrud, A., and Hassan, H. A., "Study of High-Lift Configurations Using k–ζ Transition/Turbulence Model," *Journal of Aircraft*, Vol. 37, No. 6, 2000, pp. 1008–1016.

[10]Edwards, J. R., Roy, C. J., Blottner, F. G., and Hassan, H. A., "Development of a One-Equation Transition/Turbulence Model," *AIAA Journal*, Vol. 39, No. 9, 2001, pp. 1691–1698.

[11]Kroll, N., Rossow, C. C., Becker, K., and Thiele, F., "The MEGAFLOW Project," *Aerospace Science and Technology*, Vol. 4, No. 4, 2000, pp. 223–237.

[12]Krumbein, A., and Stock, H. W., "Laminar-turbulent Transition Modeling in Navier–Stokes Solvers Using Engineering Methods," *ECCOMAS 2000* [CD-ROM], International Center for Numerical Methods in Engineering, Barcelona, Spain, Depósito Legal: B-37139-2000, 2000.

[13]Krumbein, A., "Coupling of the DLR Navier–Stokes Solver FLOWer with an e^N-Database Method for Laminar–Turbulent Transition Prediction on Airfoils," *New Results in Numerical and Experimental Fluid Mechanics III*, Notes on Numerical Fluid Mechanics, Vol. 77, Springer-Verlag, Berlin, 2002, pp. 92–99.

[14]Krumbein, A., "Transitional Flow Modeling and Application to High-Lift Multi-Element Airfoil Configurations," *Journal of Aircraft*, Vol. 40, No. 4, 2003, pp. 786–794.

[15]Krumbein, A., "Automatic Transition Prediction and Application to High-Lift Multi-Element Airfoil Configurations," *Journal of Aircraft* (to be published); also AIAA Paper 2004-2543, June/July 2004.

[16]Kroll, N., Rossow, C.-C., Schwamborn, D., Becker, K., and Heller, G., "MEGAFLOW—A Numerical Flow Simulation Tool For Transport Aircraft Design," *International Council of the Aeronautical Sciences, Congress 2002* [CD-ROM], ICAS, Toronto, 2002, pp. 1.105.1–1.105.20.

[17]Nebel, C., Radespiel, R., and Wolf, T., "Transition Prediction for 3D Flows Using a Reynolds-Averaged Navier–Stokes Code and N-Factor Methods," AIAA Paper 2003-3593, 2003.

[18]Ceresola, N., Conway, S., Eisfeld, B., Grundestam, O., Jirasek, A., Krumbein, A., Schatz, M., Thiele, F., and Wallin, S., "Implementation of Transition/turbulence Models," D3.1-2, DLR, German Aerospace Center, Rept. HiAer D3.1-2, Brunswick, Germany, April 2004.

[19]Krumbein, A., "Navier–Stokes Airfoil Computations with Automatic Transition Prediction Using the DLR TAU Code—A Sensitivity Study," Notes on Numerical Fluid Mechanics (to be published) Springer-Verlag, Berlin; also *14th Symposium of the Section 'Flows with Separation (STAB)' of the German Society of Aeronautics and Astronautics (DGLR)*, Nov. 2004.

[20]Manie, F., Piccin, O., and Ray, J. P., "Test Report of the 2D Model M1 in the ONERA F1 Wind Tunnel," GARTEUR High Lift Action Group AD (AG-08), Rept. TP041, ONERA, Chatillon, France, Oct. 1989.

[21]Arthur, M. T., Dol, H., Krumbein, A., Houdeville, R., and Ponsin, J., "Application of Transition Criteria in Navier–Stokes Computations," GARTEUR Transition Action Group AD (AG-35), Rept. TP137, ONERA, Toulouse, France, Jan. 2003.

[22]Spalart, P. R., and Allmaras, S. R., "A One-Equation Turbulence Model for Aerodynamic Flows," *La Recherche Aérospatiale*, No. 1, 1994, pp. 5–21.

[23]Edwards, J. R., and Chandra, S., "Comparison of Eddy Viscosity—Transport Turbulence Models for Three-Dimensional, Shock-Separated Flowfields," *AIAA Journal*, Vol. 34, No. 4, 1996, pp. 756–763.

[24]Wilcox, D. C., "Reassessment of the Scale-Determining Equation for Advanced Turbulence Models," *AIAA Journal*, Vol. 26, No. 11, 1988, pp. 1299–1310.